Pasteurella multocida Toxin-Stimulated Osteoclast Differentiation Is B Cell Dependent[∇]

Dagmar Hildebrand, Klaus Heeg, and Katharina F. Kubatzky*

*Universitätsklinikum Heidelberg, Department für Infektiologie, Medizinische Mikrobiologie und Hygiene,
Im Neuenheimer Feld 324, D-69120 Heidelberg, Germany*

***Pasteurella multocida* is a Gram-negative bacillus that infects a number of wild and domestic animals, causing respiratory diseases. Toxigenic *Pasteurella multocida* strains produce a protein toxin (PMT) that leads to atrophic rhinitis in swine due to enhanced osteoclastogenesis and the inhibition of osteoblast function. We show that PMT-induced osteoclastogenesis is promoted by an as-yet-uncharacterized B-cell population. The toxin, however, is not acting at the level of hematopoietic stem cells, since purified CD117$^+$ cells from murine hematopoietic progenitor cells cultivated with PMT did not mature into osteoclasts. The early macrophages contained within this cell population (CD117$^+$/CD11b$^+$) did not further differentiate into osteoclasts but survived and were able to phagocytose. Within the CD117$^-$ population, however, we detected PMT-induced generation of a B220$^+$/CD19$^+$ and B220$^+$/IgM$^+$ B-cell population that was able to take up fluorescently labeled PMT. Using purified B-cell and macrophage populations, we show that these B cells are needed to efficiently generate osteoclasts from macrophages. Cells of the immune system are thought to affect osteoclast formation and function by secreting cytokines and growth factors. We show here that PMT-stimulated B cells produce elevated levels of the osteoclastogenic factors interleukin-1β (IL-1β), IL-6, tumor necrosis factor alpha, and receptor activator of nuclear factor receptor ligand (RANKL) compared to B cells generated through incubation with IL-7. These results suggest that the osteoclastic properties characteristic for PMT may result from a cross talk between bone cells and lymphoid cells and that B cells might be an important target of *Pasteurella multocida*.**

Pasteurella multocida belongs to the group of Gram-negative bacteria and has been isolated from chronic respiratory infections in various wild and domestic animals (13, 19). Toxigenic *Pasteurella multocida* strains secrete a 146-kDa protein toxin, PMT, that is taken up by host cells through receptor-mediated endocytosis (10, 40). In pigs, *Pasteurella multocida* causes atrophic rhinitis characterized by PMT-stimulated osteoclastic bone resorption at the nasal turbinates (12) and inflammation of the nasal mucosa (24). The cellular targets of PMT are the heterotrimeric G proteins Gα$_q$, Gα$_{13}$, and Gα$_i$ (36, 37, 58, 61), which PMT renders constitutively active through deamidation of a conserved glutamine residue to glutamate (38). PMT is a known mitogen for a variety of cell types such as fibroblasts (44), bladder epithelial cells (18), or osteoclasts (30). Activation of intracellular host cell signaling cascades downstream of the heterotrimeric G proteins may lead to proliferation (26) or protection from apoptosis (41). Although many of the PMT-modulated signaling cascades have been identified, it is still under investigation whether these changes eventually elicit immunomodulation of the host.

Although the detailed mechanism of PMT on osteoclast activity is largely unknown, phenotypically, PMT induces the differentiation of preosteoclasts into osteoclasts (22, 30), eventually causing increased bone resorption of nasal turbinates. In addition, PMT seems to inhibit effective bone regeneration through osteoblasts (33). In mammalians, bone cells regulate the integrity of the skeleton, while the immune system controls the detection and destruction of invading pathogens. Interestingly, there is a strong cross talk between these two systems that led scientists to define the emerging field of osteoimmunology (3, 31). The bone-destroying osteoclasts are multinucleated cells that form from the fusion of mononuclear precursor cells developed from macrophages and are therefore hematopoietic cells. Osteoblasts, on the other hand, originate from mesenchymal progenitor cells that have the potential to differentiate into stromal cells or adipocytes (5). Differentiation of myeloid precursor cells into osteoclasts is stimulated by hematopoietic growth factors such as granulocyte-macrophage colony-stimulating factor, macrophage colony-stimulating factor, and the osteoclastogenic factors interleukin-1 (IL-1), IL-6, and tumor necrosis factor alpha (TNF-α) from stroma, monocytes, and lymphoid cells (17, 29, 39). The receptor activator of NF-κB ligand (RANKL), a member of the TNF ligand family, is produced by osteoblasts and marrow stromal cells, as well as T and B cells (23), and plays a central role in osteoclastogenesis. RANKL attaches to its receptor RANK on the cell surface of osteoclasts and osteoclast precursors, stimulating proliferation and differentiation of the cells into osteoclasts and also osteoclast survival (27, 51, 59).

In our studies we aimed to investigate how the bacterial toxin PMT can induce osteoclastogenesis and whether it disturbs bone homeostasis by stimulating the secretion of molecules with a known regulatory function in osteoclast formation. In summary, we found that murine primary bone marrow-

* Corresponding author. Mailing address: Department für Infektiologie, Medizinische Mikrobiologie und Hygiene, Im Neuenheimer Feld 324, D-69120 Heidelberg, Germany. Phone: 49-6221-5638361. Fax: 49-6221-568011. E-mail: kubatzky@uni-heidelberg.de.

derived B cells are a target of PMT and that catalytically active toxin causes the expansion of B cells. These cells secrete the osteoclastogenic factors IL-1β, IL-6, and TNF-α and show elevated mRNA and protein expression levels of the RANKL. Therefore, the B lymphocytes strongly support PMT-induced differentiation of macrophages into mature osteoclasts. Our results give a first mechanistic description of the effects of PMT on murine hematopoietic progenitor cells and add to the understanding of the physiological cross talk between bone cells and the immune system.

MATERIALS AND METHODS

Antibodies. Antibodies were obtained from BD Biosciences (anti-mouse CD117-PE, CD11b-APC, CD11b-fluorescein isothiocyanate [FITC], and B220-APC antibodies; secondary antibodies anti-rat-phycoerythrin [PE], and anti-rat-FITC), eBioscience (anti-mouse CD115), ImmunoTools (anti-mouse CD3ζ-PE, B220-PE, Gr.1, CD4-PE, CD62L-PE, CD25-PE, and CD11b-PE), BioLegend (anti-mouse RANK-PE), and Santa Cruz Biotechnologies (anti-mouse RANKL and osteopontin [OPN]).

Cell culture. Bone marrow cells were isolated from the femur of 6 to 12 weeks old C57BL/6 mice. Mixed bone marrow cells (3×10^6 cells/ml) were cultured up to 14 days in RPMI 1640 medium (Biochrom AG), containing 20% cytokine-free fetal bovine serum (FBS; ES-Cult-Hematopoietic Differentiation; Cell Systems) and 1% Pen/Strep (PAA Laboratories). Cells were stimulated with a single dose of 6.5 nM PMT^{wt} per 7 days. After 7 days fresh medium was added (1/4 of the volume).

Cell sorting. CD117$^+$, B220$^+$, and CD11b$^+$ cells were selected from bone marrow cells by using MicroBeads (Miltenyi Biotec) according to the manufacturer's protocol and performing the AutoMACS POSSEL program (Miltenyi Biotec). Purity was determined by fluorescence-activated cell sorting (FACS) staining with anti-mouse CD117-PE, anti-mouse CD11b-PE, or anti-mouse B220-PE antibodies and analysis with a BD FACSCanto workstation and BD FACSDiva software (BD Biosciences).

Hematoxylin and eosin staining. Paraformaldehyde (4%)-fixed cytospin bone marrow cells treated for 7 days with PMT^{wt} (6.5 nM) or left unstimulated were incubated with hematoxylin (Mayer's Haemalaun, T865.1; Roth) for 10 min at room temperature to stain the nucleus. After being washed with water, the cells were incubated with eosin (0.5% aqueous Eosin G solution; Roth) for 15 min at room temperature to stain the cytoplasm. For microscopy (Leica Microsystems GmbH), cytospins were mounted with glycerin–phosphate-buffered saline (PBS; Merck) and covered with a coverslip.

Measurement of cell viability. Bone marrow cell survival was determined by quantification of cellular ATP using the Cell Titer Glo assay (Promega). A total of 5×10^4 cells/ml were seeded in a 96-well plate and stimulated with PMT^{wt}, heat inactivated PMT^{wt} ΔT (65°C, 15 min), the catalytically inactive mutant PMT^{C1165S} (all 6.5 nM) or left unstimulated. After 7 days cells were processed according to the manufacturer's protocol, and the luminescence was determined by using a LUMIstar Optima luminometer and Optima reader control software (BMG Labtech).

Flow cytometry (FACS). Briefly, cells were washed with PBS–10% FBS, blocked for 30 min in PBS–10% FBS, and incubated with the corresponding antibodies in PBS–10% FBS for 1 h at 4°C. After three washes with PBS–10% FBS, cells that were stained with an unlabeled primary antibody were incubated with the appropriate secondary antibody for 30 min at 4°C and washed again three times. Quantification was done by FACS analysis using a BD FACSCanto workstation and BD FACSDiva software (BD Biosciences).

PMT labeling. Recombinantly produced PMT (8) was labeled with fluorescent Atto-647 (ATTO-TEC). A portion (1 mg) of PMT was dialyzed (Slide-A-Lyzer dialysis cassette; Thermo Scientific) against 10 mM PBS (pH 8.3). The amine-reactive dye was dissolved in anhydrous dimethyl sulfoxide, and the concentration was determined photometrically. The protein was incubated with a 2-fold molar excess of reactive dye for 1 h at room temperature in the dark. Free dye was removed by gel filtration (Column PD-10 [GE Healthcare] with Sephadex G-50 [Sigma-Aldrich]). The column was preequilibrated with PBS (10 mM, pH 8.3) and labeled PMT was eluted by centrifugation at $100 \times g$.

PMT uptake assay. Freshly prepared bone marrow cells were incubated with Atto-647-labeled PMT for 4 h at 37°C. After the cells were washed five times with PBS, FACS analysis was performed with antibodies against cell-type-specific surface markers, such as Gr-1 (granulocytes), CD117 (stem cells), CD3ζ, CD25, CD4 (T cells), B220 and IgM (B cells), CD11b (macrophages), CD62 (endothe-

lial cells), and Ter119 (erythroid cells). FACS analysis was performed using a BD FACSCanto workstation and BD FACSDiva software (BD Biosciences).

Phagocytosis assay. PMT^{wt} bone marrow cells were stimulated for 6 days before incubation with yellow-green fluorescent latex beads (#L4530; Sigma-Aldrich) for 30 min at 37°C. As controls, cells and beads were either incubated at 4°C (negative control) or macrophages (positive control). Macrophages were generated by selection of bone marrow cells for 6 days with 30% L929 cell conditioned medium (L929-CM) (2). After four washes with PBS, the amount of phagocytosed fluorescent beads was quantified by using a BD FACSCanto workstation and BD FACSDiva software (BD Biosciences).

Quantitative real-time PCR. B220$^+$ and B220$^-$ bone marrow cells were stimulated with PMT^{wt} (6.5 nM) for 4 or 6 days or with 10 ng of IL-7 (NatuTec)/ml for 5 days. RNA was extracted by using a High-Pure RNA isolation kit (Roche) according to the manufacturer's protocol. CDNA was prepared by using a Revert Aid First-Strand cDNA synthesis kit (Fermentas). Aliquots of the cDNA were subjected to quantitative reverse transcription-PCR (RT-PCR) analysis using SYBR Green Rox mix (Thermo Scientific) with the following primers: GAPDH, sense (5′-TCCCATTCTTCCACCTTTGATG-3′) and antisense (5′-GTCCACC ACCCTGTTGCTGTA-3′; murine RANKL, sense (5′-AGCCGAGACTACGG CAAGTA-3′) and antisense (5′-GCGCTCGAAAGTACAGGAAC-3′); murine IL-6, sense (5′-AACGATGATGCACTTGCAGA-3′) and antisense (5′-CTCTG AAGGACTCTGGCTTTG-3′); murine TNF-α, sense (5′-AAAATTCGAGTG ACAAGCCTGTAG-3′) and antisense (5′-CCCTTGAAGAGAGAACCTGGG AGTAG-3′); murine IL-1β, sense (5′-ACTCATTGTGGCTGTGGAGAAG-3′) and antisense (5′-GCCGTCTTTCATTACACAGGAC-3′); murine actin, sense (5′-CCCTGTGCTGCTCACCGA-3′) and antisense (5′-ACAGTGTGGGTGA CCCCCTC-3′); and murine Cathepsin K, sense (5′-ATGTGGGGGCTCAAG GTTCTG-3′) and antisense (5′-CATATGGGAAAGCATCTTCAGAGT-3′). The results were analyzed by using the Fast Real-Time PCR system (Applied Biosystems). All results were normalized with respect to the reference genes *GAPDH* or *actin*.

Enzyme-linked immunosorbent assay (ELISA). Isolated B220$^+$ cells were treated for 5 days with 10 ng of IL-7 or 6.5 nM PMT^{wt}/ml. To measure the secretion of IL-1β, IL-6, and TNF-α, enzyme-linked immunosorbent assays (ELISAs) were performed according to the manufacturer's protocol (BD OptEIA mouse IL-1β, mouse IL-6, and mouse TNF-α ELISA SET). Assays were quantified with the microplate reader Sunrise and Magellan software (Tecan).

Coculture experiments. B220$^+$ cells and CD11b$^+$ cells were selected by AutoMACS cell purification. From these purifications, five different fractions were generated: BMC mix (without isolation), B220$^+$ cells (positive cells from B220$^+$ isolation), B220$^-$ cells (negative cells from B220$^+$ isolation), CD11b$^+$ cells (positive cells from CD11b$^+$ isolation), CD11b$^-$ cells (negative cells from CD11b$^+$ isolation), and the B220$^-$/CD11b$^-$ cell fraction (CD11b depletion and subsequent B200 removal). After 14 days of PMT^{wt} stimulation, cells were stained for the osteoclast marker RANK and analyzed by using a BD FACSCanto workstation and BD FACSDiva software (BD Biosciences).

RESULTS

Studies on the signal transduction of the toxin in mammalian host cells show that the *Pasteurella multocida* toxin PMT is a potent mitogen (44). It was established that PMT influences the differentiation of macrophages, which are osteoclast progenitor cells, into mature osteoclasts (16), but it is unknown what triggers this differentiation process. We therefore investigated how PMT influences the differentiation of murine hematopoietic progenitor cells.

To investigate whether PMT has effects on cells other than direct osteoclast progenitors, we prepared total bone marrow cells containing hematopoietic progenitor cells from C57BL/6 mice. The harvested mixed progenitor cells were cultivated for 7 days in the presence or absence of PMT^{wt} in cytokine-free medium. A cytospin and subsequent hematoxylin and eosin staining were performed to investigate the morphology of the cells microscopically. While cells left untreated (Fig. 1A, left panel) had mostly died, bone marrow cells cultivated with PMT^{wt} had produced two distinct populations (right panel). Although the larger cells (~20 μm) resembled macrophages
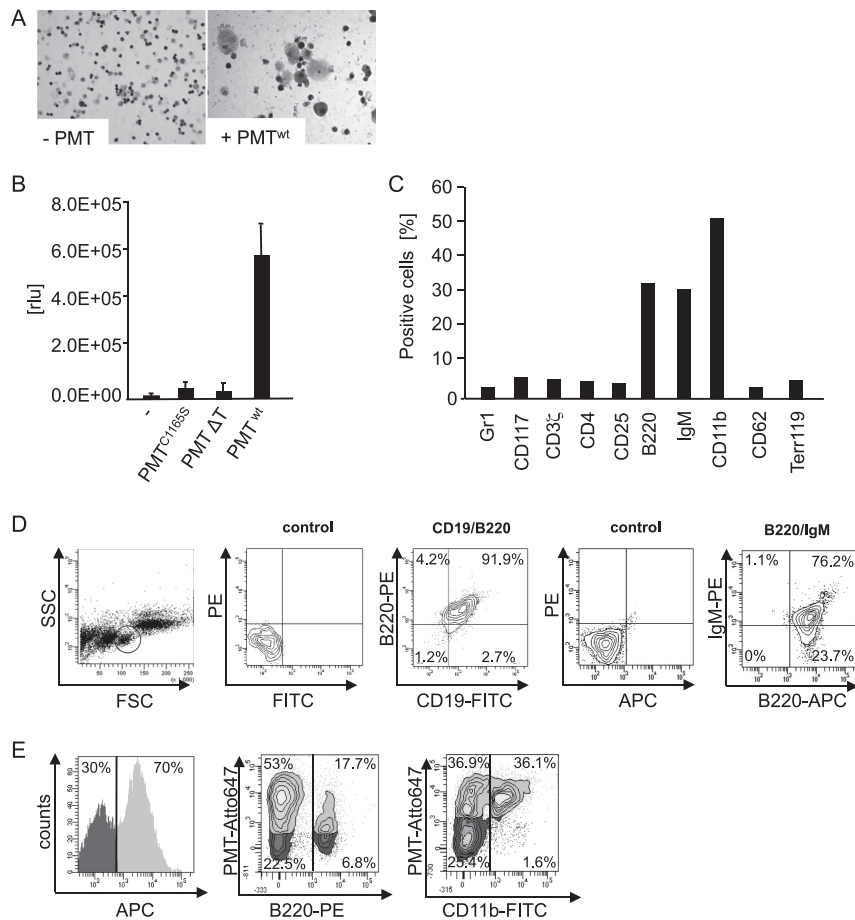
FIG. 1. PMT induces the differentiation of murine hematopoietic bone marrow cells into B cells and macrophages. (A) Morphological analysis of bone marrow cells. Cytospins of bone marrow cells stimulated with PMTwt (6.5 nM) and untreated cells were paraformaldehyde fixed, stained with hematoxylin and eosin, and mounted with glycerin-PBS for microscopy. (B) Measurement of PMT-induced cell viability. Cell survival was determined by performing Cell Titer Glo assays. Cells (5×10^4 cells/ml) were seeded in a 96-well plate and stimulated with PMTwt, PMTC1165S, or heat-inactivated PMT ΔT (all 6.5 nM) or left unstimulated. After 7 days, the cell viability was determined in an ATP-based luminescence assay. The indicated standard deviation (SD) was calculated from three independent experiments with duplicates (mean ± SD; $n = 3$). (C) FACS analysis of specific surface markers. Bone marrow cells were stimulated for 6 days with 6.5 nM PMTwt and stained with cell-specific surface markers. Gr-1 (granulocytes), CD117 (stem cells), CD3ζ, CD25, CD4 (T cells), B220 and IgM (B cells), CD11b (macrophages), CD62 (endothelial cells), and Ter119 (erythroid cells) were evaluated. (D) Characterization of B cells. PMTwt-stimulated (6 days, 6.5 nM) bone marrow cells were double stained for the B-cell markers B220 and CD19 or for B220 and IgM, respectively. (E) Uptake of fluorescently labeled PMTwt. PMTwt was labeled with Atto-647 and incubated with murine bone marrow cells for 4 h before FACS analysis. PMTwt uptake by all cells (left panel), B220+ cells (middle), and CD11b+ cells (right panel) was determined by FACS analysis. Panels A, C, D, and E show representative results from at least two independent experiments.

from their size and morphology, smaller, round cells were also detectable (~10 μm). To investigate whether the catalytic activity of PMT was required for this effect, we used an inactive mutant PMTC1165S (57) that contains a mutation in the catalytic center of the toxin (38). In addition, we tested heat-inactivated PMTwt (65°C, 16 min) to exclude contaminations by bacterial cell wall components such as lipopolysaccharide (LPS) during the preparation of recombinant toxin (8). Toxin activity was assessed by measuring cell survival through quantification of cellular ATP using a Cell Titer Glo assay. To that end, 5×10^4 cells/ml were seeded in a 96-well plate and stimulated with PMTwt, PMTC1165S, heat-inactivated PMT (PMT ΔT), or left unstimulated. After 7 days, quantification of viable cells showed that only treatment with PMTwt had a significant stimulating effect on bone marrow cell proliferation

(Fig. 1B). Since PMTC1165S or heat-inactivated PMT-stimulated bone marrow cells died during cultivation, we only used cytokine-free culture conditions as a negative control in the following experiments.

In order to unambiguously identify the cell populations detected in Fig. 1A, we used a number of lineage-specific surface markers, such as Gr-1 (granulocytes), CD117 (stem cells), CD3ζ, CD4, and CD25 (T cells), B220 and IgM (B cells), CD11b (macrophages), CD62 (endothelial cells), and Ter119 (erythroid cells) to characterize the cells by FACS analysis. Figure 1C summarizes our results as a graph and shows that only three of the antibodies used tested positive, namely, the B-cell-specific markers B220 and IgM, as well as CD11b, a marker for macrophages. To date, only macrophages and osteoclasts have been reported to be generated after incubation

of bone marrow cells with PMT, thus we wanted to corroborate our finding that PMT[wt] causes the expansion of bone marrow-derived B cells. In the subsequent double staining with the typical B-cell markers B220 and CD19, we found at least 90% of the cells within the lymphoid cell population (left panel) to express these markers (Fig. 1C). Next, we purified B220^{+} cells from PMT-treated bone marrow cells using MACS cell purification and performed a double staining with anti-B220 and an antibody against IgM, as the most specific marker for B cells. More than 75% of all B220^{+} cells express IgM on their surface, which thus can be unambiguously identified as immature B cells. The approximately 25% of cells that are positive for B220 but negative for IgM are probably more immature cells and may represent pro- or pre-B cells.

To verify that these two cell populations, identified as B cells and macrophages, were targets of PMT, we produced fluorescently labeled PMT (PMT Atto-647) and verified the uptake of PMT by FACS analysis. Murine bone marrow cells were prepared and incubated with PMT for 4 h. Approximately 70% of all living cells present took up PMT (Fig. 1D, left panel). To detect the specific uptake of PMT by B cells and macrophages, we identified the respective cells by B220 or CD11b staining (middle and right panel). A total of 70% of the B220[+] population (i.e., 17.7% of all cells) were able to take up PMT. Macrophages on the other hand represented ca. 36% of the bone marrow mix, and all of these cells were able to take up PMT. Whether this is due to receptor-mediated uptake by which the toxin is known to enter cells or due to phagocytosis cannot be clarified from these experiments. Furthermore, we determined the uptake of PMT by other hematopoietic cells to investigate whether these cells that were not present after PMT selection had not been able to take up PMT or whether these cells initially took up the toxin but did not survive. Ter119^{+}, CD62^{+}, CD117^{+}, Gr-1^{+} bone marrow cell and splenic CD4^{+} T cells also have the ability to take up PMT to a varying extent (data not shown).

When we investigated the macrophage containing cell population for CD11b expression, we found 95% of these cells (circle in left panel) stained positive for macrophages (Fig. 2A). To characterize these cells in a functional assay, we performed a phagocytosis assay using FITC-labeled latex beads. As a positive control, macrophages were generated by culturing bone marrow cells for 6 days in RPMI 1640 medium containing 30% L929 cell conditioned medium. Both PMT[wt] and L929-CM differentiated cells were able to phagocytose the labeled beads to the same extent, as detected by FACS analysis for FITC-positive cells (Fig. 2B). To check whether the macrophages could be further differentiated into osteoclasts, a mixed preparation of murine bone marrow cells was incubated with PMT[wt] and checked for the development of osteoclasts after 10 to 14 days of incubation. At that time, cells with typical osteoclast morphology had formed and were detectable as large, multinuclear cells (~40 μm) that contained extensive vacuoles (Fig. 2C). In addition, we confirmed the formation of osteoclasts by FACS analysis using an osteoclast specific surface marker, the receptor activator of nuclear factor receptor RANK (Fig. 2D). While the left panel shows an increase in cell size and granularity between cells after 7 days (Fig. 2A, left panel) and those cultivated for 14 days (Fig. 2D, left panel), the right panel of Fig. 2D shows that at that time ca. 44% of the cell population is RANK positive. To corroborate this, we
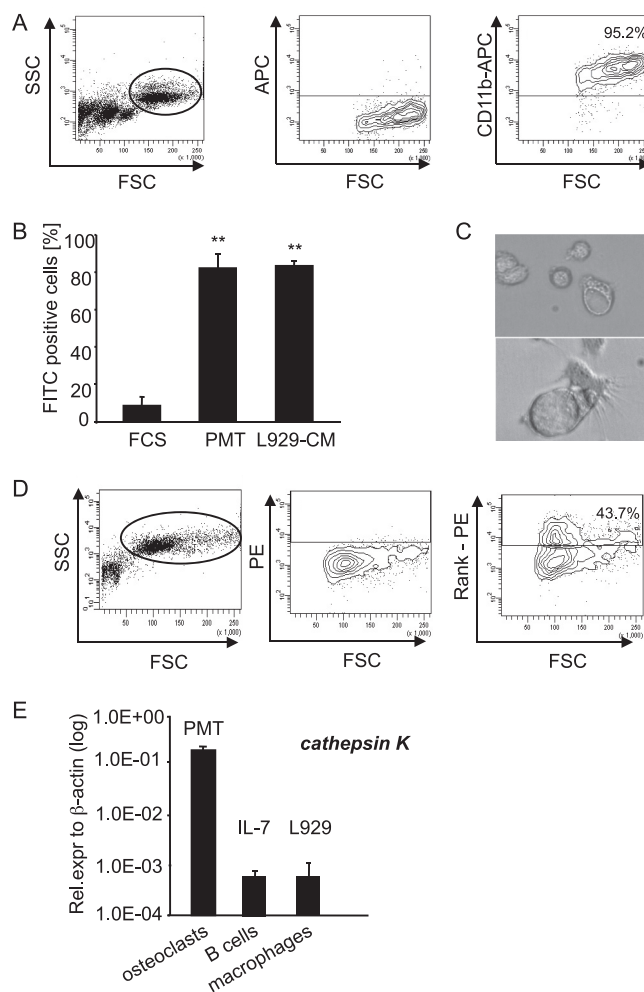

FIG. 2. PMT-derived macrophages phagocytose and have the potential to differentiate into osteoclasts. (A) Characterization of macrophages. PMT[wt]-stimulated (6 days, 6.5 nM) bone marrow cells were stained for the macrophage marker CD11b. The right panel shows staining of the gated macrophage population. (B) Functional characterization of the macrophage population. Bone marrow cells stimulated for 6 days with PMT[wt] and untreated bone marrow cells were incubated with FITC-labeled latex beads at 37°C or at 4°C (negative control). As a positive control macrophages were used that had been generated by selection of bone marrow cells with L929 conditioned medium. The CD11b-containing population was analyzed for FITC-positive cells. The diagram shows the percentage of FITC positive cells minus values of negative controls. The indicated standard deviation was calculated from three independent experiments (mean ± SD; $n =$ 3). The statistical significance was assessed by using a paired Student t test (∗∗, $P < 0.01$). (C) Characterization of osteoclasts. A mixed preparation of murine bone marrow cells was incubated with 6.5 nM PMT[wt] for 14 days. Osteoclasts were identified by their typical morphology. (D) RANK expression. The formation of osteoclasts was analyzed by FACS using the osteoclast specific surface marker RANK. The right panel shows the staining of the gated population in the left panel, and the middle panel shows unstained control cells. (E) Transcription level of the osteoclastic marker *cathepsin K*. The amounts of *cathepsin K* after PMT[wt] treatment (6.5 nM, 12 days), IL-7-generated B cells (10 ng/ml, 5 days), and L929-generated macrophages (30% L929-CM, 6 days) were analyzed by quantitative RT-PCR using *cathepsin K*-specific primers and normalization to *actin* expression. The indicated SD was calculated from two independent experiments (mean ± SD; $n = 2$).
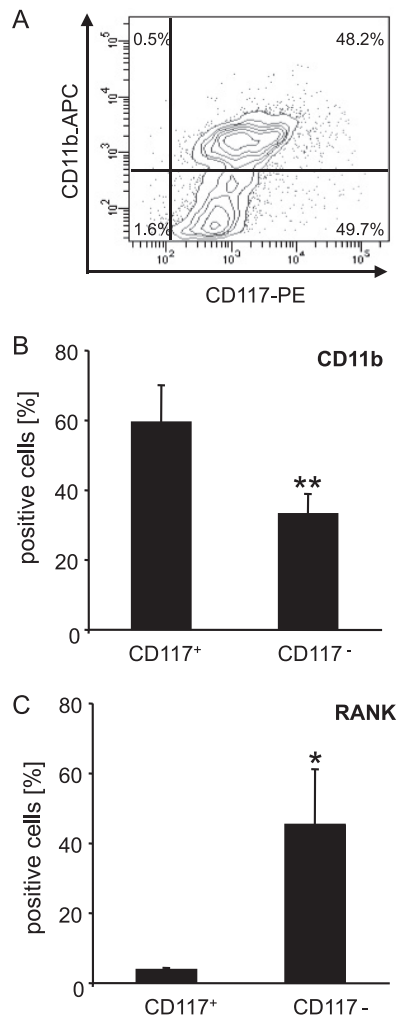
FIG. 3. Differentiation of CD117$^+$ and CD117$^-$ fractions cultivated with PMT. (A) Purification of CD117$^+$ stem cells. Stem cell receptor (CD117) expressing cells from a mix of total bone marrow cells were purified by MACS purification technology, double stained for CD117 and CD11b, and analyzed by FACS. (B and C) Quantification of macrophages and osteoclasts in CD117$^+$ and CD117$^-$ cells. After 9 days of stimulation with PMT^{wt} (6.5 nM), the amounts of CD11b$^+$ macrophages (B) and RANK$^+$ osteoclasts (C) from the CD117$^+$ and CD117$^-$ fractions were quantified by FACS analysis with specific antibodies. The indicated SD was calculated from three independent experiments (mean ± SD; $n = 3$). The statistical significance was assessed by using a paired Student t test (∗, $P < 0.05$; ∗∗, $P < 0.01$).
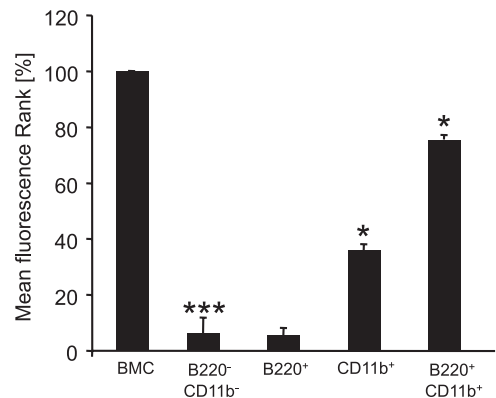

FIG. 4. PMT-induced osteoclast generation is B-cell dependent. FACS staining of osteoclasts was performed. Uisng MACS cell purification of B220$^+$ cells or CD11b$^+$ cells or purification of both cell types, five different fractions (BMC mix, B220$^-$ CD11b$^-$, B220$^+$, CD11b$^+$, and B220$^+$ CD11b$^+$ cells) were generated. After 14 days of PMT^{wt} stimulation, the cells were stained for the osteoclast marker RANK and analyzed by FACS. The results of the mean fluorescence of RANK-positive cells from two independent experiments, normalized to osteoclasts derived from bone marrow cells (100%), are shown. The indicated SD was calculated from the two experiments and is presented as a percentage of the control value (mean ± SD; $n = 2$). The statistical significance was assessed by using a paired Student t test (∗, $P < 0.05$; ∗∗∗, $P < 0.005$).

analyzed the cells for expression of the *cathepsin K* gene since this lysosomal cysteine protease is predominantly found in osteoclasts (54). Figure 2E shows that after 12 days of stimulation with PMT^{wt} the generated osteoclasts have a 200-fold higher expression of *cathepsin K* than B cells selected with IL-7 or L929-CM selected macrophages that were used as controls (Fig. 2E). In summary, the data prove the generation of osteoclasts through treatment of bone marrow cells with PMT^{wt}.

To determine whether PMT^{wt} modulates hematopoietic cell differentiation at the level of hematopoietic stem cells and early progenitors, we purified stem cell receptor (CD117)-expressing cells from murine bone marrow cells, before adding PMT^{wt}. The CD117$^+$ population initially contained ca. 48% of CD11b$^+$ cells (Fig. 3A), which represent early macrophage

progenitor cells that stain positive for both CD11b and CD117 (49). There were no B cells detectable in this cell fraction, as detected by FACS analysis using a B220 antibody (data not shown). After 9 days of differentiation, the amount of macrophages and osteoclasts from the CD117$^+$ and CD117$^-$ fraction was quantified by FACS analysis (Fig. 3B and C). In the CD117$^+$ sample, the CD11b$^+$ cells now represented ca. 60% of all viable cells. However, these cells had not differentiated into osteoclasts (Fig. 3C), nor did we detect further differentiation at later time points (data not shown), as controlled by the detection of RANK-positive cells. We therefore conclude that the CD117$^+$ fraction of cells contained a high number of immature macrophage progenitors that were maintained and probably expanded in the presence of PMT^{wt}, without induction of cell differentiation. However, when the CD117$^-$ population was characterized, we found a significantly smaller number of macrophages at day 9 of PMT^{wt} cultivation (ca. 33%) but a large number of RANK-positive cells (45.2% versus 3.6% in CD117$^+$ cells) (Fig. 3B and C).

Since the cell population sorted for CD117 expression did not contain any of the B cells that had been present after cultivation of unsorted bone marrow preparations, we hypothesized that the absence of B cells might be responsible for the inability of the CD117$^+$ population to efficiently generate osteoclasts. We therefore systematically depleted or enriched for B cells and macrophage populations using MACS cell purification and determined the generation of RANK-expressing osteoclasts after 14 days by FACS analysis. Figure 4 shows a summary of the results from two independent experiments wherein the fluorescence of RANK-positive cells was determined and normalized to the RANK expression in osteoclasts derived from bone marrow cells (BMC). Depletion of both B cells and macrophages completely inhibited generation of os-

teoclasts (6%). While B cells alone did not produce osteoclasts (5%), CD11b$^+$ macrophages alone were able to produce a significant increase in the amount of osteoclasts (35%) compared to the positive control. However, only when we used a combination of purified B cells and macrophages was osteoclastogenesis efficient, yielding a RANK fluorescence of 75% of the positive control. Whether this decrease in RANK mean fluorescence in the B220$^+$/CD11b$^+$ population compared to our positive control (BMC) (75% versus 100%) was caused by the absence of stimulatory factors from other cells, or whether the purification procedure did not allow to restore the osteoclastic potential completely remained unclear.

Since it is known that cells of the immune system are able to influence osteoclast formation by secreting osteoclastic proteins, we further investigated whether PMT manipulates B cells so that they produce increased levels of osteoclastogenic factors. It is known that activated B lymphocytes secrete proinflammatory cytokines such as IL-1β, IL-6, and TNF-α that are of great importance for osteoclast development (20, 25, 45). We therefore performed quantitative real-time PCR to determine the amounts of cytokine mRNA in cells stimulated for 5 days with PMT^{wt} or IL-7, as described in Materials and Methods. Figure 5A shows that PMT^{wt} stimulates an increase in IL-1β, IL-6, and TNF-α expression. The expression levels of IL-1β and IL-6 are 10 and 15-fold higher, respectively, compared to IL-7, while the expression levels of TNF-α was comparable between IL-7-generated and PMT^{wt}-stimulated cells. ELISAs of supernatants obtained from these B cells corroborated the results also on the protein level and revealed an elevated secretion of IL-1β, IL-6, and TNF-α (Fig. 5B). B cells also produce RANKL, another TNF-α family member that stimulates differentiation of early osteoclast progenitors into mature osteoclasts (42). *RANKL* expression was investigated using cells that were positive or negative for B220$^+$. Cells were stimulated for up to 6 days with PMT^{wt} and RNA was extracted at days 0, 4, and 6. As a control, IL-7-generated B cells were used, since IL-7 is known to induce expression of RANKL (52). While the B-cell-negative cells (B220$^-$) did not express RANKL, PMT^{wt}-treated B220 cells (B220$^+$) expressed RANKL to levels comparable to IL-7-selected B cells. To confirm these data at the protein level, we performed FACS analysis using a RANKL-specific antibody and a PE-labeled secondary antibody. The histogram overlay of RANKL expression (Fig. 5D) shows that IL-7- and PMT-treated cells highly express RANKL and that the expression levels are comparable. Since RANKL is also expressed on the surface of osteoblasts (4), we wanted to exclude the possibility that the B220$^+$ cell population contained osteoblasts. We therefore stained cells obtained after purification with B220 magnetic beads (B220$^+$) with an antibody against OPN, a protein specifically expressed on osteoblasts (60). As a positive control, we used the rat osteosarcoma cell line ROS 17/2.8. FACS analysis revealed that whereas ROS 17/2.8 cells express OPN (Fig. 5E, left panel), B220$^+$ selected cells are OPN negative (Fig. 5E, right panel) and are therefore free of any osteoblast impurity.

DISCUSSION

In this study we set out to define the process of osteoclast differentiation induced by *Pasteurella multocida* toxin. Since

the bone destructive effect of PMT in atrophic rhinitis is a very striking phenotype, PMT is characterized as a toxin primarily acting on osteoclasts and osteoblasts. Therefore, many researchers focused on the effect of PMT on these specific cells (12, 30, 32, 50), and only limited information is available on the effect of PMT on other hematopoietic cells. Jutras et al. showed that PMT is able to stimulate osteoclastogenesis of mononuclear, adherent murine bone marrow cells from mice (22), suggesting that PMT acts on early osteoclast progenitor cells, such as macrophages that then differentiate into mature osteoclasts. However, these authors did not provide details on the mechanisms of this process. Using a porcine bone marrow differentiation model, Gwaltney et al. also report that fluorescently labeled PMT was mostly found in small round cells that did not appear to be macrophages or osteoclasts but rather resembled lymphoid cells (16). Our data verify this hypothesis and, in cell cultures obtained from murine bone marrow cells cultivated with PMT in the absence of additional cytokines, we detected CD11b$^+$ macrophages, RANK$^+$ osteoclasts, as well as B220$^+$/CD19$^+$ and B220$^+$/IgM$^+$ B cells. The uptake of PMT was detectable in both B cells and macrophages, as well as in other immune cells.

The comparatively new field of osteoimmunology investigates the cross talk between cells of the skeleton and the immune system (28). It is hypothesized that perturbation of lymphoid cell differentiation can ultimately affect bone formation. It is therefore an intriguing question whether the known osteoclastic properties of this bacterial toxin result from PMT-induced changes of the lymphoid system rather than directly acting on the bone cells itself. This is supported by our findings that immature macrophages (CD117$^+$/CD11b$^+$) themselves are not able to undergo further differentiation in the presence of PMT and that macrophages (CD11b$^+$) differentiate significantly more efficient in the presence of B cells (Fig. 4B). In addition, we show that these B cells produce increased amounts of cytokines, such as IL-1β, IL-6, TNF-α, or RANKL, compared to IL-7-selected B cells. The cytokines detected are proinflammatory or osteoclastic cytokines, and aberrant expression of these cytokines has been linked to various human bone diseases. IL-1β, or osteoclast activating factor, was the first cytokine being linked to bone resorption in idiopathic and postmenopausal osteoporosis (21), and IL-1β, TNF-α, and IL-6 also play a critical role in several autoimmune diseases such as rheumatoid arthritis, spongyloarthropathies, osteomyelitis, or lupus erythematosus (1, 15, 46). However, IL-1β, TNF-α, and RANKL not only promote osteoclast activity and osteoclastogenesis but also act as inhibitors of bone-growing osteoblasts (14, 34, 47). Interestingly, PMT too, was described to have an inhibitory effect on the function of osteoblastic cells (32). Therefore, the question whether PMT is more important for osteoclasts or osteoblasts might have to be discussed taking into account that both cell types are targets for factors secreted by the lymphoid system.

Apart from the inflammatory processes described above, tumors can contribute to osteolysis, for example, through bone lytic metastases (1); the most frequent cancer directly affecting the skeleton, however, is the plasma B-cell cancer multiple myeloma, where ca. 90% of the patients develop bone lesions (43). It is also discussed that multiple myeloma cells might have osteoclastic potential or form multinucleated osteoclast-
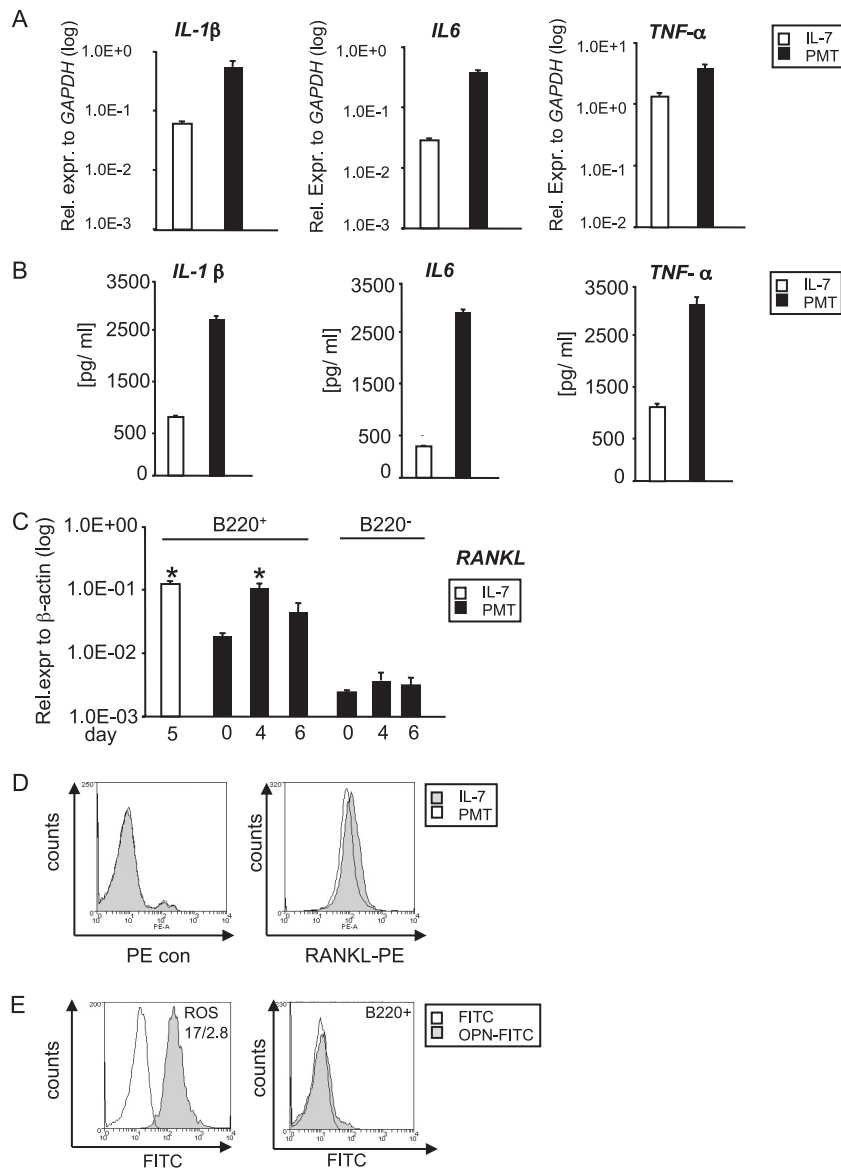
FIG. 5. Production of osteoclastic cytokines. (A and B) Detection of mRNA and protein levels of osteoclastic cytokines. (A) The induction of *IL-1β*, *IL-6*, and *TNF-α* gene expression was determined in IL-7-generated B cells (10 ng/ml, 5 days) and PMT^wt-treated (6.5 nM, 5 days) B220^+ B cells. (B) In addition, the secretion of these cytokines was measured by using the corresponding ELISA. Shown are representative results from at least three different experiments. (C) *RANKL* transcription levels. *RANKL* expression of B220^+ and B220^- cells was analyzed by quantitative RT-PCR using *RANKL*-specific primers and normalization to *actin* expression. The indicated SD was calculated from two independent experiments (mean ± SD; $n = 2$). Statistical significance of *RANKL* expression changes compared to samples on day 0 were assessed by using a paired Student t test (∗, $P < 0.05$). (D) RANKL protein expression levels. The surface expression of RANKL on IL-7- and PMT-treated B220^+ cells was analyzed by flow cytometry using an anti-RANKL and a PE-labeled secondary antibody. As a control, cells were stained with secondary antibody only. (E) OPN expression. B220^+ selected cells were stained with an osteopontin (OPN)-specific antibody and an FITC-labeled secondary antibody (right panel). As a positive control, ROS17/2.8 cells were used (left panel). The overlays in panels D and E were produced using Weasel v2.5 software.

like cells (9, 48), and it is clear that these cells show an up-regulated secretion of osteoclastic factors such as TNF-α, RANKL, and IL-6 (11). The similarities to the phenotype we observed in PMT-treated B cells are remarkable and exist also on the level of molecular signaling events. Recently, we described PMT as a very potent antiapoptotic agent that upregulates the survival kinases Pim-1 and Akt, as well as a number of antiapoptotic molecules, such as Bcl-2 family members (41).

Multiple myeloma cells also fail to undergo apoptosis and accumulate in the bone marrow due to the upregulated expression of antiapoptotic molecules such as Bcl-2, Bcl-xL, and Mcl-1 and the decreased expression of proapoptotic molecules (55). In addition, constitutive Akt and STAT3 activation was found in myeloma cell lines and patient cells, whereas these proteins were not found in nonmalignant hematopoietic cells from the same patient or in plasma cells from healthy individ-

uals (7, 53). The issue of whether PMT has immunomodulatory properties has been discussed by many researchers with respect to results obtained from vaccination studies. Despite the general structural similarity to other AB toxins such as cholera toxin or pertussis toxin, PMT was shown to be a poor adjuvant and to be able to suppress the mucosal adjuvant activity of cholera toxin (6). Considering the fact that the immunogenicity of PMT increases when it is used as a toxoid (35, 56), the existing data suggest that catalytically active PMT downregulates the host's immune response, and our studies highlight the importance of B cells as a target of PMT.

In the future it will be of great interest to identify the complete secretome produced by immune cells during PMT stimulation in order to determine the molecular events of PMT-induced osteoclastogenesis. It can be anticipated that PMT might be a valuable tool that could enable us to increase our understanding on the interplay between B cells and osteoclasts and to gain new insights into the development of human bone diseases.

ACKNOWLEDGMENTS

REFERENCES

1. **Abu-Amer, Y.** 2009. Inflammation, cancer, and bone loss. Curr. Opin. Pharmacol. **9:**427–433.
2. **Akagawa, K. S., K. Kamoshita, and T. Tokunaga.** 1988. Effects of granulocyte-macrophage colony-stimulating factor and colony-stimulating factor-1 on the proliferation and differentiation of murine alveolar macrophages. J. Immunol. **141:**3383–3390.
3. **Arron, J. R., and Y. Choi.** 2000. Bone versus immune system. Nature **408:** 535–536.
4. **Atkins, G. J., P. Kostakis, B. Pan, A. Farrugia, S. Gronthos, A. Evdokiou, K. Harrison, D. M. Findlay, and A. C. Zannettino.** 2003. RANKL expression is related to the differentiation state of human osteoblasts. J. Bone Miner. Res. **18:**1088–1098.
5. **Aubin, J. E.** 2001. Regulation of osteoblast formation and function. Rev. Endocrinol. Metab. Disord. **2:**81–94.
6. **Bagley, K. C., S. F. Abdelwahab, R. G. Tuskan, and G. K. Lewis.** 2005. *Pasteurella multocida* toxin activates human monocyte-derived and murine bone marrow-derived dendritic cells in vitro but suppresses antibody production in vivo. Infect. Immun. **73:**413–421.
7. **Bharti, A. C., S. Shishodia, J. M. Reuben, D. Weber, R. Alexanian, S. Raj-Vadhan, Z. Estrov, M. Talpaz, and B. B. Aggarwal.** 2004. Nuclear factor-κB and STAT3 are constitutively active in CD138⁺ cells derived from multiple myeloma patients, and suppression of these transcription factors leads to apoptosis. Blood **103:**3175–3184.
8. **Blocker, D., L. Berod, J. W. Fluhr, J. Orth, M. Idzko, K. Aktories, and J. Norgauer.** 2006. *Pasteurella multocida* toxin (PMT) activates RhoGTPases, induces actin polymerization and inhibits migration of human dendritic cells, but does not influence macropinocytosis. Int. Immunol. **18:**459–464.
9. **Calvani, N., P. Cafforio, F. Silvestris, and F. Dammacco.** 2005. Functional osteoclast-like transformation of cultured human myeloma cell lines. Br. J. Haematol. **130:**926–938.
10. **Dudet, L. I., P. Chailler, J. D. Dubreuil, and B. Martineau-Doize.** 1996. *Pasteurella multocida* toxin stimulates mitogenesis and cytoskeleton reorganization in Swiss 3T3 fibroblasts. J. Cell Physiol. **168:**173–182.
11. **Ehrlich, L. A., and G. D. Roodman.** 2005. The role of immune cells and inflammatory cytokines in Paget's disease and multiple myeloma. Immunol. Rev. **208:**252–266.
12. **Felix, R., H. Fleisch, and P. L. Frandsen.** 1992. Effect of *Pasteurella multocida* toxin on bone resorption in vitro. Infect. Immun. **60:**4984–4988.
13. **Foged, N. T.** 1992. *Pasteurella multocida* toxin. The characterisation of the toxin and its significance in the diagnosis and prevention of progressive atrophic rhinitis in pigs. APMIS Suppl. **25:**1–56.
14. **Gilbert, L., X. He, P. Farmer, S. Boden, M. Kozlowski, J. Rubin, and M. S. Nanes.** 2000. Inhibition of osteoblast differentiation by tumor necrosis factor-alpha. Endocrinology **141:**3956–3964.
15. **Goldring, S. R.** 2003. Pathogenesis of bone and cartilage destruction in rheumatoid arthritis. Rheumatology (Oxford) **42**(Suppl. 2)**:**ii11–ii16.
16. **Gwaltney, S. M., R. J. Galvin, K. B. Register, R. B. Rimler, and M. R. Ackermann.** 1997. Effects of *Pasteurella multocida* toxin on porcine bone marrow cell differentiation into osteoclasts and osteoblasts. Vet. Pathol. **34:**421–430.
17. **Heymann, D., J. Guicheux, F. Gouin, N. Passuti, and G. Daculsi.** 1998. Cytokines, growth factors, and osteoclasts. Cytokine **10:**155–168.
18. **Hoskins, I. C., L. H. Thomas, and A. J. Lax.** 1997. Nasal infection with *Pasteurella multocida* causes proliferation of bladder epithelium in gnotobiotic pigs. Vet. Rec. **140:**22.
19. **Hunt, M. L., B. Adler, and K. M. Townsend.** 2000. The molecular biology of *Pasteurella multocida.* Vet. Microbiol. **72:**3–25.
20. **Ibelgaufts, H.** 1995. Dictionary of cytokines. VCH Publishers, Inc., Weinheim, Germany.
21. **Jandinski, J. J.** 1988. Osteoclast activating factor is now interleukin-1β: historical perspective and biological implications. J. Oral Pathol. **17:**145–152.
22. **Jutras, I., and B. Martineau-Doize.** 1996. Stimulation of osteoclast-like cell formation by *Pasteurella multocida* toxin from hemopoietic progenitor cells in mouse bone marrow cultures. Can. J. Vet. Res. **60:**34–39.
23. **Kawai, T., T. Matsuyama, Y. Hosokawa, S. Makihira, M. Seki, N. Y. Karimbux, R. B. Goncalves, P. Valverde, S. Dibart, Y. P. Li, L. A. Miranda, C. W. Ernst, Y. Izumi, and M. A. Taubman.** 2006. B and T lymphocytes are the primary sources of RANKL in the bone resorptive lesion of periodontal disease. Am. J. Pathol. **169:**987–998.
24. **Kimman, T. G., C. W. Lowik, L. J. van de Wee-Pals, C. W. Thesingh, P. Defize, E. M. Kamp, and O. L. Bijvoet.** 1987. Stimulation of bone resorption by inflamed nasal mucosa, dermonecrotic toxin-containing conditioned medium from *Pasteurella multocida*, and purified dermonecrotic toxin from *P. multocida.* Infect. Immun. **55:**2110–2116.
25. **Lahat, N., E. Aghai, B. Maroun, A. Kinarty, M. Quitt, and P. Froom.** 1991. Increased spontaneous secretion of IL-6 from B cells of patients with B chronic lymphatic leukaemia (B-CLL) and autoimmunity. Clin. Exp. Immunol. **85:**302–306.
26. **Lax, A. J., G. D. Pullinger, M. R. Baldwin, D. Harmey, A. E. Grigoriadis, and J. H. Lakey.** 2004. The *Pasteurella multocida* toxin interacts with signalling pathways to perturb cell growth and differentiation. Int. J. Med. Microbiol. **293:**505–512.
27. **Leibbrandt, A., and J. M. Penninger.** 2008. RANK/RANKL: regulators of immune responses and bone physiology. Ann. N. Y. Acad. Sci. **1143:**123–150.
28. **Lorenzo, J., M. Horowitz, and Y. Choi.** 2008. Osteoimmunology: interactions of the bone and immune system. Endocrinol. Rev. **29:**403–440.
29. **Manolagas, S. C., and R. L. Jilka.** 1995. Bone marrow, cytokines, and bone remodeling: emerging insights into the pathophysiology of osteoporosis. N. Engl. J. Med. **332:**305–311.
30. **Martineau-Doize, B., I. Caya, S. Gagne, I. Jutras, and G. Dumas.** 1993. Effects of *Pasteurella multocida* toxin on the osteoclast population of the rat. J. Comp. Pathol. **108:**81–91.
31. **Mensah, K. A., J. Li, and E. M. Schwarz.** 2009. The emerging field of osteoimmunology. Immunol. Res. **45:**100–113.
32. **Mullan, P. B., and A. J. Lax.** 1996. *Pasteurella multocida* toxin is a mitogen for bone cells in primary culture. Infect. Immun. **64:**959–965.
33. **Mullan, P. B., and A. J. Lax.** 1998. *Pasteurella multocida* toxin stimulates bone resorption by osteoclasts via interaction with osteoblasts. Calcif. Tissue Int. **63:**340–345.
34. **Nguyen, L., F. E. Dewhirst, P. V. Hauschka, and P. Stashenko.** 1991. Interleukin-1β stimulates bone resorption and inhibits bone formation in vivo. Lymphokine Cytokine Res. **10:**15–21.
35. **Nielsen, J. P., N. T. Foged, V. Sorensen, K. Barfod, A. Bording, and S. K. Petersen.** 1991. Vaccination against progressive atrophic rhinitis with a recombinant *Pasteurella multocida* toxin derivative. Can. J. Vet. Res. **55:**128–138.
36. **Orth, J. H., I. Fester, I. Preuss, L. Agnoletto, B. A. Wilson, and K. Aktories.** 2008. Activation of Gαᵢ and subsequent uncoupling of receptor-Gαᵢ signaling by *Pasteurella multocida* toxin. J. Biol. Chem. **283:**23288–23294.
37. **Orth, J. H., S. Lang, M. Taniguchi, and K. Aktories.** 2005. *Pasteurella multocida* toxin-induced activation of RhoA is mediated via two families of Gα proteins, Gαq and Gα12/13. J. Biol. Chem. **280:**36701–36707.
38. **Orth, J. H., I. Preuss, I. Fester, A. Schlosser, B. A. Wilson, and K. Aktories.** 2009. *Pasteurella multocida* toxin activation of heterotrimeric G proteins by deamidation. Proc. Natl. Acad. Sci. U. S. A. **106:**7179–7184.
39. **Pacifici, R.** 1996. Estrogen, cytokines, and pathogenesis of postmenopausal osteoporosis. J. Bone Miner. Res. **11:**1043–1051.
40. **Pettit, R. K., M. R. Ackermann, and R. B. Rimler.** 1993. Receptor-mediated binding of *Pasteurella multocida* dermonecrotic toxin to canine osteosarcoma and monkey kidney (Vero) cells. Lab. Invest. **69:**94–100.
41. **Preuss, I., D. Hildebrand, J. H. C. Orth, K. Aktories, and K. F. Kubatzky.** 2010. *Pasteurella multocida* toxin is a potent activator of antiapoptotic signalling pathways. Cell Microbiol. doi:10.1111/j.1462-5822.2010.01462.x.

42. **Robinson, L. J., C. W. Borysenko, and H. C. Blair.** 2007. Tumor necrosis factor family receptors regulating bone turnover: new observations in osteoblastic and osteoclastic cell lines. Ann. N. Y. Acad. Sci. **1116:**432–443.

43. **Roodman, G. D.** 2009. Pathogenesis of myeloma bone disease. Leukemia **23:**435–441.

44. **Rozengurt, E., T. Higgins, N. Chanter, A. J. Lax, and J. M. Staddon.** 1990. *Pasteurella multocida* toxin: potent mitogen for cultured fibroblasts. Proc. Natl. Acad. Sci. U. S. A. **87:**123–127.

45. **Sati, H. I., M. Greaves, J. F. Apperley, R. G. Russell, and P. I. Croucher.** 1999. Expression of interleukin-1 beta and tumour necrosis factor-alpha in plasma cells from patients with multiple myeloma. Br. J. Haematol. **104:**350–357.

46. **Schett, G.** 2008. Review: immune cells and mediators of inflammatory arthritis. Autoimmunity **41:**224–229.

47. **Sezer, O.** 2009. Myeloma bone disease: recent advances in biology, diagnosis, and treatment. Oncologist **14:**276–283.

48. **Silvestris, F., S. Ciavarella, M. De Matteo, M. Tucci, and F. Dammacco.** 2009. Bone-resorbing cells in multiple myeloma: osteoclasts, myeloma cell polykaryons, or both? Oncologist **14:**264–275.

49. **Simmons, P. J., G. W. Aylett, S. Niutta, L. B. To, C. A. Juttner, and L. K. Ashman.** 1994. c-Kit is expressed by primitive human hematopoietic cells that give rise to colony-forming cells in stroma-dependent or cytokine-supplemented culture. Exp. Hematol. **22:**157–165.

50. **Sterner-Kock, A., B. Lanske, S. Uberschar, and M. J. Atkinson.** 1995. Effects of the *Pasteurella multocida* toxin on osteoblastic cells in vitro. Vet. Pathol. **32:**274–279.

51. **Tanaka, S., K. Nakamura, N. Takahasi, and T. Suda.** 2005. Role of RANKL in physiological and pathological bone resorption and therapeutics targeting the RANKL-RANK signaling system. Immunol. Rev. **208:**30–49.

52. **Toraldo, G., C. Roggia, W. P. Qian, R. Pacifici, and M. N. Weitzmann.** 2003. IL-7 induces bone loss in vivo by induction of receptor activator of nuclear factor κB ligand and tumor necrosis factor alpha from T cells. Proc. Natl. Acad. Sci. U. S. A. **100:**125–130.

53. **Tu, Y., A. Gardner, and A. Lichtenstein.** 2000. The phosphatidylinositol 3-kinase/AKT kinase pathway in multiple myeloma plasma cells: roles in cytokine-dependent survival and proliferative responses. Cancer Res. **60:**6763–6770.

54. **Vaananen, H. K., and T. Laitala-Leinonen.** 2008. Osteoclast lineage and function. Arch. Biochem. Biophys. **473:**132–138.

55. **van de Donk, N. W., H. M. Lokhorst, and A. C. Bloem.** 2005. Growth factors and antiapoptotic signaling pathways in multiple myeloma. Leukemia **19:**2177–2185.

56. **van Diemen, P. M., G. de Vries Reilingh, and H. K. Parmentier.** 1994. Immune responses of piglets to *Pasteurella multocida* toxin and toxoid. Vet. Immunol. Immunopathol. **41:**307–321.

57. **Ward, P. N., A. J. Miles, I. G. Sumner, L. H. Thomas, and A. J. Lax.** 1998. Activity of the mitogenic *Pasteurella multocida* toxin requires an essential C-terminal residue. Infect. Immun. **66:**5636–5642.

58. **Wilson, B. A., X. Zhu, M. Ho, and L. Lu.** 1997. Pasteurella multocida toxin activates the inositol triphosphate signaling pathway in *Xenopus* oocytes via $G_q\alpha$-coupled phospholipase C-β1. J. Biol. Chem. **272:**1268–1275.

59. **Xing, L., E. M. Schwarz, and B. F. Boyce.** 2005. Osteoclast precursors, RANKL/RANK, and immunology. Immunol. Rev. **208:**19–29.

60. **Yamate, T., H. Mocharla, Y. Taguchi, J. U. Igietseme, S. C. Manolagas, and E. Abe.** 1997. Osteopontin expression by osteoclast and osteoblast progenitors in the murine bone marrow: demonstration of its requirement for osteoclastogenesis and its increase after ovariectomy. Endocrinology **138:**3047–3055.

61. **Zywietz, A., A. Gohla, M. Schmelz, G. Schultz, and S. Offermanns.** 2001. Pleiotropic effects of *Pasteurella multocida* toxin are mediated by Gq-dependent and -independent mechanisms. involvement of Gq but not G11. J. Biol. Chem. **276:**3840–3845.